Research Article

Vasu Sujitha, Kadarkarai Murugan, Chellasamy Panneerselvam*, Al Thabiani Aziz, Fuad A. Alatawi, Subrata Trivedi, Zuhair M. Mohammedsaleh, Hatem A. Al-Aoh, Fayez M. Saleh, Suhair A. Bani-Atta, Giulia Bonacucina, and Filippo Maggi

Fabrication of green nanoinsecticides from agri-waste of corn silk and its larvicidal and antibiofilm properties

https://doi.org/10.1515/gps-2022-0062
received November 11, 2021; accepted March 30, 2022

Abstract: The corn silk (CS) is composed of the thread-like stigmas of female inflorescences of *Zea mays* L. and represents an important waste material from maize crop production that can be recycled in further applications. In this research, the CS was used for the bio-fabrication of Ag nanoparticles (AgNPs) that were evaluated against (I–V) larval instars and pupae of the mosquito vector *Aedes aegypti*. CS-AgNPs were characterized by UV-Vis spectroscopy, TEM, EDAX, XRD, FTIR, DLS, and zeta potential analysis. *Z. mays* extract analyzed by gas chromatography mass spectrometry reveals 14 compounds. The larvicidal effectiveness of CS-fabricated AgNPs was 2.35 $\mu g \cdot mL^{-1}$ (I Instar) to 6.24 $\mu g \cdot mL^{-1}$ (pupae). The field application in water storage reservoirs of both CS extracts and CS-AgNPs ($10 \times LC_{50}$) led to a 68–69% reduction in larval density after 72 h post-treatment. Ecotoxicological impact of CS-fabricated AgNPs was evaluated on the predatory efficacy of *Poecilia reticulata* on all the larval instars and pupae of *Ae. aegypti*. Finally, CS-AgNPs were tested to elucidate its anti-biofilm attributes. The CS-AgNPs at 125 $\mu g \cdot mL^{-1}$ showed a biofilm inhibition of 90% on *S. aureus* and 79% on *S. epidermidis*. These results support the use of CS-AgNPs for futuristic green alternative to mosquito vector management.

Keywords: *Aedes aegypti*, *Poecilia reticulata*, silver nanoparticles, anti-biofilm, *Zea mays* silk

1 Introduction

Mosquito-borne diseases like malaria, dengue, and filariasis account for global mortality and morbidity with increased resistance to conventional insecticides [1–4]. As an alternative, green methods have evolved to augment the control of deadly mosquitoes. An endemic disease, dengue, is mainly transmitted by *Aedes aegypti* and *Aedes albopictus*. However, chemical control of dengue vector involves not only high operational costs but also sustains adverse effect on nontarget organisms. The development of insect pests which are resistant to synthetic drugs has created the need for developing alternative approaches using materials extracted from plants, including the agro wastes [5,6]. Plants are store house of secondary metabolites playing an important ecological role as insecticides and promising alternative to conventional mosquito larvicides [7,8]. Agro waste-mediated metal nanoparticles are of interest due to their environmental compatibility and various applications on an industrial level [9]. Phyto-mediated nanomaterials can be prepared cheaply and easily [10–13]. Corn silk (CS) is an abundant waste formed while producing

* **Corresponding author: Chellasamy Panneerselvam,** Department of Biology, Faculty of Science, University of Tabuk, Tabuk 71491, Saudi Arabia, e-mail: cpselva@ymail.com
Vasu Sujitha: Department of Zoology, Division of Entomology, School of Life Sciences, Bharathiar University, Coimbatore 641 046, Tamil Nadu, India
Kadarkarai Murugan: Department of Zoology, Division of Entomology, School of Life Sciences, Bharathiar University, Coimbatore 641 046, Tamil Nadu, India; NMV University, 182/2, Bypass Road, Poonamallee, Chennai 600 056, India
Al. Thabiani Aziz, Fuad A. Alatawi: Department of Biology, Faculty of Science, University of Tabuk, Tabuk 71491, Saudi Arabia
Subrata Trivedi: School of Health and Applied Sciences, Apex Professional University NH-52, Pesighat Smart City, Arunachal Pradesh 791102, India
Zuhair M. Mohammedsaleh: Department of Medical Laboratory Technology, Faculty of Applied Medical Sciences, University of Tabuk, Tabuk 71491, Saudi Arabia
Hatem A. Al-Aoh, Suhair A. Bani-Atta: Department of Chemistry, Faculty of Science, University of Tabuk, Tabuk 71491, Saudi Arabia
Fayez M. Saleh: Department of Medical Microbiology, Faculty of Medicine, University of Tabuk, Tabuk 71491, Saudi Arabia
Giulia Bonacucina, Filippo Maggi: School of Pharmacy, University of Camerino, Camerino, Italy

sweet corn and from food processing industries [14]; CS showed both antimicrobial and antibiotic activities [15]. Flavonol glycosides present in CS act as antioxidants and are used for diabetes management [16]. Bacteria employ to form biofilm, that is enclosed by an exopolysaccharide (EPS) to improve their survival by increasing antimicrobial resistance. The Center for Disease Control and Prevention estimates that biofilms are responsible for over 65% of all chronic bacterial infections [17]. Therefore, the validation of alternative approaches is needed for the control of mosquito and bacterial pathogens [8]. Controlling of mosquito larvae by natural predators such as insects and small vertebrates like larvivorous fishes is eco-friendly and has high efficacy to limit mosquito populations [18]. We investigated the predatory efficiency of freshwater guppy, *Poecilia reticulata* Peters against different larval instars of *Ae. aegypti*. Interestingly, the *Z. mays*-fabricated silver nanoparticles (AgNPs) boosting the predatory efficacy of guppy on *Ae. aegypti* is investigated. In the present investigation, after developing CS-mediated AgNPs, we evaluated their contact toxicity against different larval stages of *Ae. aegypti*. The bio-fabricated CS-AgNPs were characterized using various biophysical techniques. Furthermore, we evaluated the effects of sublethal doses of CS-AgNPs on the predatory behavior of *P. reticulata* on *Ae. aegypti* under laboratory conditions. For comparative purposes, we also tested the CS extract. Given the ability of several types of nanomaterials to inhibit microbial-derived biofilm [19], we also evaluated the anti-biofilm properties of CS-AgNPs on *Staphylococcus aureus* and *S. epidermidis*.

2 Materials and methods

2.1 Collection of CS and methanol extraction

Zea mays L. silk was procured from agricultural firms of Udumalaipettai, which is located at Tiruppur District, Tamil Nadu. It was validated by Taxonomist of Botanical Survey of India, whose reference number was BSI/SRC/5/23/2019/Tech./4 and deposited at Department of Zoology, Bharathiar University, Coimbatore, Tamil Nadu, India. Double distilled water (DDH_2O) was used to clean the silk threads which was further dried away from the sunlight at 28 ± 2°C. Two hundred and fifty grams of silk threads were extracted for a time span of 72 h using absolute methanol by employing Soxhlet apparatus. A 20% yield was obtained, which was maintained at 4°C for future use.

2.2 Production and characterization of CS-fabricated AgNPs

AgNPs were prepared according to Murugan et al. [20] with minor changes following Sasidharan et al. [21]. In order to prepare the nanoparticles, 10 mL of CS extract was allowed to react with 90 mL of 1 mM $AgNO_3$ for a time span of four hours.

The absorption curve of AgNPs was obtained by UV-Vis spectrophotometry (UV-3600 spectrometer, Shimadzu, Japan). Transmission electron microscopy was done by TEM-JEOL model instrument 1200 EX, Japan, operating at 10 kV and energy dispersive X-ray spectroscopy by EDX-JEOL mode 6390, Japan. FTIR was performed using a Perkin–Elmer spectrum 2000 FTIR, USA. XRD results were obtained using Phillips PW1830 equipment [22].

2.3 GC–MS analysis of CS extract

GC–MS analysis has been acquired on a Clarus 500 Perkin–Elmer gas chromatograph with a Turbo mass gold-Perkin–Elmer detector. The column dimensions were 30 m × 0.25 mm × 0.25 µm with the 5% diphenyl/95% dimethyl poly siloxane stationary phase column. For GC–MS detection, an electron ionization system with an ionization energy of 70 eV was used. Helium gas (99.99%) was used as the carrier gas at a constant flow rate of 1 mL·min^{-1} and an injection volume of 3 mL was employed (split ratio of 10:1). Injector temperature was 250°C; ion-source temperature was 280°C. The oven temperature was programed from 110°C (isothermal for 2 min), with an increase of 10°C·min^{-1} to 200°C (no hold), then from 5°C·min^{-1} to 280°C, ending with a 9 min isothermal at 280°C. Mass spectra were taken at 70 eV, a scan interval of 0.5 s and fragments from 45 to 450 Da. Total GC running time was 36 min. The relative percentage amount of each component was calculated by comparing its average peak area to the total areas. Software adopted to handle mass spectra and chromatograms was a Turbomass version (5.2.0.2.14).

2.4 Larvicidal/pupicidal experiments in the laboratory

Each stage of larval instar and pupae of mosquitoes was reared in a sustainable way as described by Suresh et al. [23]. Twenty-five larvae of each instar and pupae were treated

with 250 mL solutions containing 249 mL of deionized H_2O and 1 mL of required concentration of CS methanolic extract (100–500 ppm) or CS-AgNPs (2–10 ppm) according to a procedure outlined by Sujitha et al. [24]. Five replicates were used for each experiment and deionized water without extract/nanoformulation was used as control; the percentage of death was calculated after 24 h of exposure.

2.5 Experiments on predation in the laboratory

Mettur Dam located in the Salem District of Tamil Nadu in India was the site for collection of Guppy fish (*Poecilia reticulata*). Acclimatization of the Guppy fishes was done in the laboratory prior to any experiment. Four hundred numbers of *Ae. aegypti* larvae (I–1V instar) were placed with one guppy fish adult in a 2 L glass tank filled with deionized water plus 1 mL of the desired concentration of the CS extract silk-mediated AgNPs. All the experiments were conducted in five replicates. Control was deionized water only. The experimental tanks were checked every 24 h at daytime and nighttime and the number of preys eaten by guppy fish was calculated. After each checking, the predated mosquito instars were replaced with new ones. Predatory efficiency was determined using the following formula:

$$\text{Predation efficiency} = \text{Number of consumed mosquitoes/Total number of mosquitoes} \times 100 \quad (1)$$

2.6 Assessing larvicidal activity in the field

Six different outdoor water bodies were used to study the larvicidal activities of bio-fabricated AgNPs and the CS extract. After 24-, 48-, and 72-h exposure, the larval density calculations were done by following the procedure of Panneerselvam et al. [25]. Lethal toxicity was assessed on third and fourth instar larvae of mosquito. Six replicates were performed maintaining 27 ± 2°C and 80% relative humidity as previously done by Panneerselvam et al. [25]. Ten times the Lethal $\text{Concentration}_{50}$ was used in accordance to Murugan et al. [26]. On the basis of surface area (0.25 m^2) and volume (250 L), the quantity of insecticide to be used was ascertained. The following formula was used to calculate the percentage of larval density reduction:

$$\text{Percentage of larval reduction} = (C - T)/C \times 100 \quad (2)$$

where C is the total number of mosquitoes in the control and T is the total number of mosquitoes in the treatment.

2.7 Anti-biofilm assay

Biofilm was formed by pouring 100 µL of trypticase soy broth with 1% glucose solutions into plates maintained at 35 ± 2°C for 24 h. About 0.9% saline solution was used to remove the unattached cells followed by staining with 2% crystal violet. Furthermore, 90 µL of trypticase soy broth and 10 µL of CS-fabricated AgNPs were added to all the parallel well biofilms. All the experiments were conducted in three sets. To elucidate biofilm inhibition potential, 100 µL of *Staphylococcus aureus* or *Staphylococcus epidermidis* in trypticase soy broth was followed by 24-h of incubation. Planktonic cells were discarded after washing. Biofilm was obtained according to the procedure outlined by Mu et al. [27] and Stefanovic and Hegde [28].

2.8 Extraction of EPS

Filtration of supernatant was accomplished using 0.22 µm nitrocellulose membrane followed by treatment with chilled absolute ethyl alcohol and incubation for 12 h at 4°C to obtain EPS as a precipitate [29]. EPS was quantified according to Dubois et al. [30].

2.9 Statistical analysis

Data were analyzed using SPSS software v. 16.0. Larval toxicity data and biofilm inhibition data were ascertained by two-way ANOVA with two factors (i.e., concentration and mosquito life stages/bacterial strains), followed by Tukey's HSD test ($P = 0.05$). Mosquito mortality data were determined by Probit analysis [31]. Two-way ANOVA was adopted to analyze mosquito larval population data from field bioassay with two factors (i.e., mosquito treatment and the elapsed time from the treatment) followed by Tukey's HSD test.

Guppy fish predation data were determined via JMP 7 using a weighted generalized linear model with two fixed factors:

$$y = X\beta + \varepsilon \quad (3)$$

where y is the vector of the observations (i.e., the number of consumed preys), X is the incidence matrix, β is the vector of fixed effects (i.e., the mosquitocidal treatment and targeted instar), and ε is the vector of random residual effect. A probability level of $P < 0.05$ was used for the significance of difference between values.

3 Results and discussion

3.1 Chemical profiling of *Z. mays* (GC-MS)

The GC-MS analysis of *Z. mays* extracts show the presence of 14 compounds as shown in Figure 1 and Table 1. For

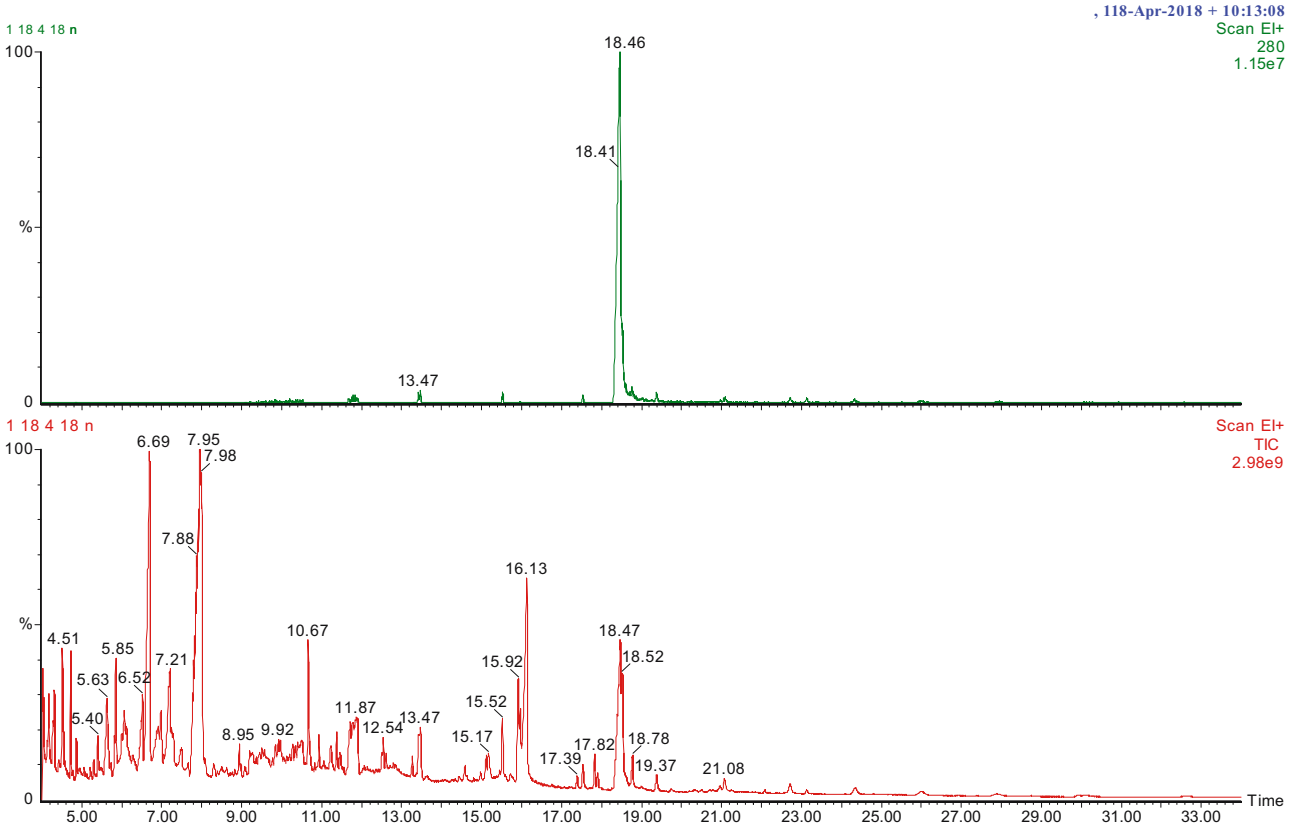

Figure 1: GC-MS spectrum of the *Z. mays* silk extract.

Table 1: Main compounds identified by GC–MS analysis in the *Z. mays* silk extract

Ht	REV	for	Compound name	MW	Formula	CAS
1	987	965	9,12-Octadecadienoic acid(*z.z*)-	280	$C_{18}H_{32}O_2$	60-33-3
2	976	884	9,12-Octadecadienoic acid (*z.z*)-	280	$C_{18}H_{32}O_2$	60-33-3
3	949	891	9,12-Octadecadienoic acid, methyl ester	294	$C_{19}H_{34}O_2$	2462-85-3
4	943	907	9,12-Octadecadienoic acid, methyl ester, (*e,e*)-	294	$C_{19}H_{34}O_2$	2566-97-4
5	937	898	1,*e*-11,*z*-13-Octadecatriene	248	$C_{18}H_{32}$	80625-36-1
6	935	856	9,12-Octadecadienoic acid, ethyl ester	308	$C_{20}H_{36}O_2$	7619-08-1
7	934	793	9,12-Octadecadienoic acid, methyl ester,(*z,z*)-	294	$C_{19}H_{34}O_2$	17309-05-6
8	930	882	9,12-Octadecadien-1-0l (*z,z*)-	266	$C_{18}H_{34}O$	506-43-4
9	928	829	9,12-Octadecadienoic acid, (*z,z*)-,methyl ester	294	$C_{19}H_{34}O_2$	112-63-0
10	928	878	9,17- Octadecadienal,(*z*)-	264	$C_{18}H_{32}O$	56554-35-9
11	927	859	*cis*-13, 16-Docasadienoic acid	336	$C_{22}H_{40}O_2$	7370-49-2
12	925	854	8,11-Octadecadienoic acid, methyl ester	294	$C_{19}H_{34}O_2$	56599-58-7
13	924	851	9,12-Octadecadienoic acid, (z,z)-,methyl ester	294	$C_{19}H_{34}O2$	112-63-0
14	922	789	Ethyl9,12hexadecadienoate	280	$C_{18}H_{32}O_2$	900336-70-1

instance, Abirami et al. [32] reported that the presence of 1-(+) ascorbic acid 2, *n*-hexadecanoic acid in the ethanol extract of CS. Comparably, the fatty acid peak profile of *Z. mays* was noticed in the chromatogram [33]. Furthermore, 9,12-octadecadienoic acid, methyl ester, and 9-octdecenoic acid methyl ester were observed in *Casimiroa edulis* La Llave and lex leaf extract with significant insecticidal and antifeedant properties on *Spodoptera littoralis* [34].

3.2 CS-AgNP synthesis and characterization

CS-fabricated AgNPs changed the color from pale yellow to dark brown at 4 h of photo period. An extreme absorption peak for AgNPs was noticed at 450 nm (Figure 2). The broadening of the peak indicated that the particles are polydispersed. Similarly, Rajkumar et al. [35] noticed that *Z. mays*-mediated AgNPs exhibited a sharp absorption peak at 420 nm. Also, Hema et al. [36] observed the maximum UV-Vis absorption peak of *Z. mays*-decorated AgNPs between 410 and 450 nm.

CS-AgNPs were either spherical or cubic in structure, with a mean size ranging between 10 and 50 nm (Figure 3). Similarly, Patra and Baek [37] noticed that the *Zea mays* L. silky hairs-fabricated AgNPs displayed spherical in shape and the size ranging from 100 to 450 nm. Furthermore, Eren and Baran [38] observed that the *Zea mays* L. leaves extract-based AgNPs exhibit the size less than 100 nm and *Zea mays* L. (corn flour) synthesized nanosilver particles showed monodispersed spherical in shape. The EDX analysis of CS-AgNPs revealed strong peaks of silver (42.4%) confirming the high purity of AgNPs (Figure 4), with the optical absorption peak at 3 keV due to surface plasmon resonance [25,35]. Also, the EDX analysis exhibited the peak of oxygen (O), indicating

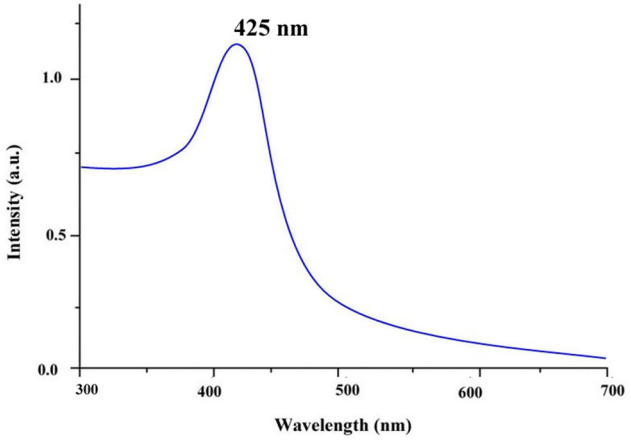

Figure 2: UV-Vis spectrum of *Z. mays* silk-fabricated AgNPs.

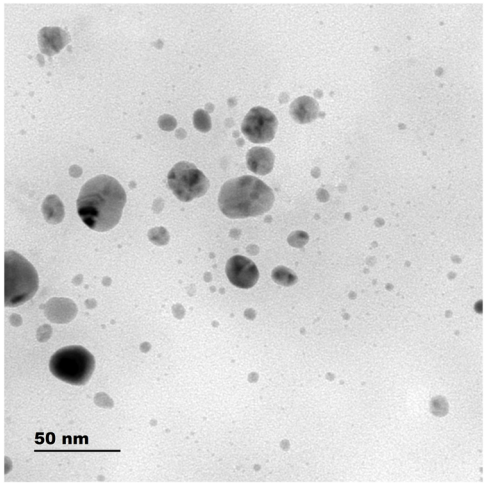

Figure 3: TEM image of *Z. mays* silk-fabricated AgNPs.

that CS-AgNPs stabilized by the presence of organic compounds in the *Z. mays* extract. This result was well matched with Chen et al. [39] who have reported results on the corn straw-synthesized AgNPs.

Figure 5 reveals the XRD pattern of *Z. mays*-synthesized AgNPs. The XRD results of *Z. mays*-synthesized AgNPs were corresponding with JCPDS card number (04–0783). The XRD patterns of CS-AgNPs exhibited strong Bragg reflections at 38.47, 44.09, 64.56, and 77.37 corresponding to the planes (111), (200), (220), and (311) (Figure 5), which well matched with the reports of Hema et al. [36], who observed that flower-shaped AgNPs from *Z. mays* had strongest diffraction peaks at 38.6° and 64°, while Rajkumar et al. [35] noticed diffraction peaks at 38.2, 44.42, 64.4, 76.7, and 81.45, which indicates the crystalline nature of AgNPs from *Z. mays*.

The FTIR spectra of AgNPs synthesized from *Z. mays* are shown in Figure 6. The synthesized AgNP spectrum reveals various characteristic peaks at 3,350, 2,974, 1,738, 1,661, and 1,273 cm^{-1}, respectively. A peak at 3,350 cm^{-1} was assigned to N–H stretching of the amine group and an observed peak at 1,661 cm^{-1} was attributed to –C═C–H stretching of alkenes. The absorption peaks at 1,378 and 2,974 cm^{-1} of AgNPs are relative to the presence of alkynes, carboxylic acids, and phenolic group [36]. The peak at 1,738 cm^{-1} corresponds to the carbonyl stretching vibration, while the peak at 1,660 cm^{-1} can be attributed to C═C stretching vibration. The peak at 1,273 cm^{-1} corresponds to the C–O stretching vibration. The slight shifting of various functional groups in the AgNPs from *Z. mays* displayed the progress of the reduction processes with capping and stabilization [40].

The zeta potential value of *Z. mays*-fabricated AgNPs was measured as –14.3.86 (Figure 7). The synthesized AgNPs

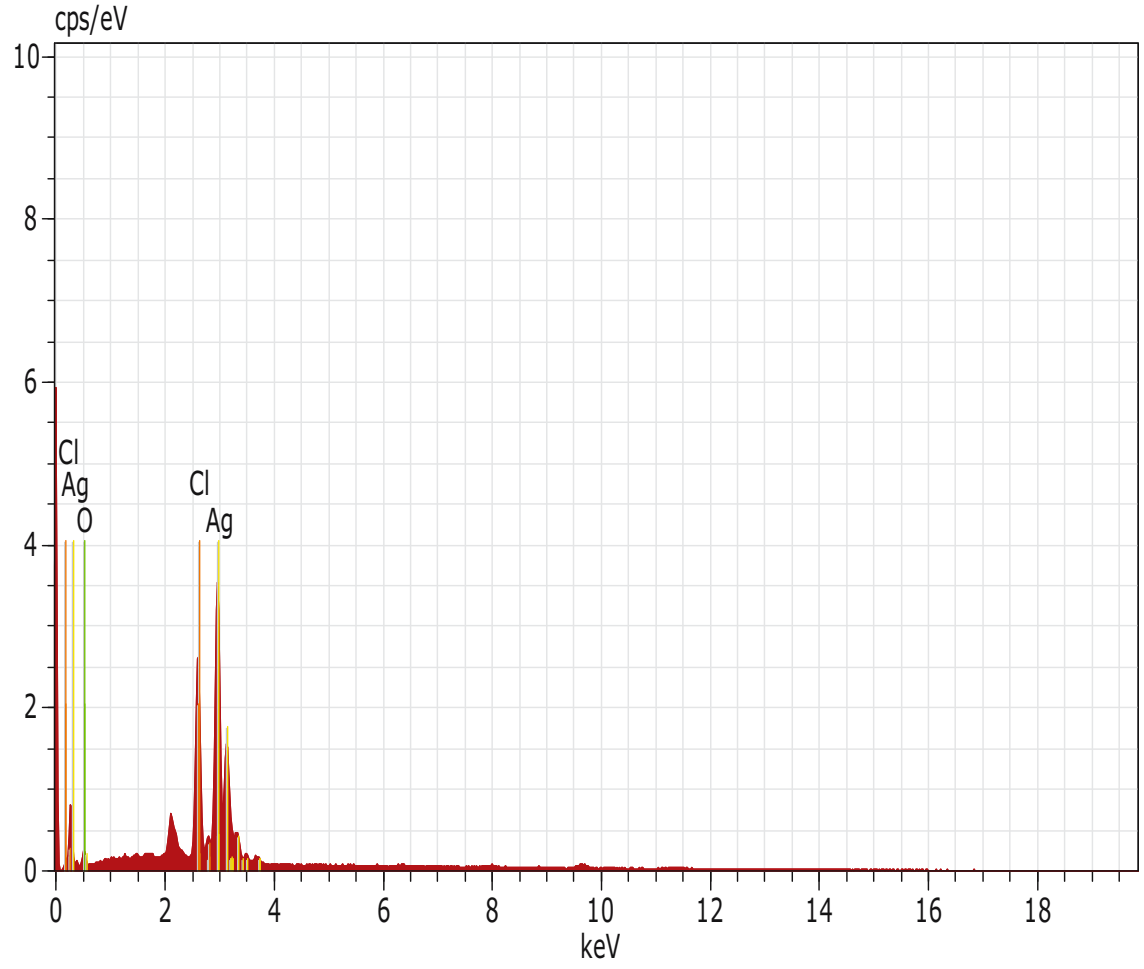

Figure 4: EDX spectrum of *Z. mays* silk-fabricated AgNPs.

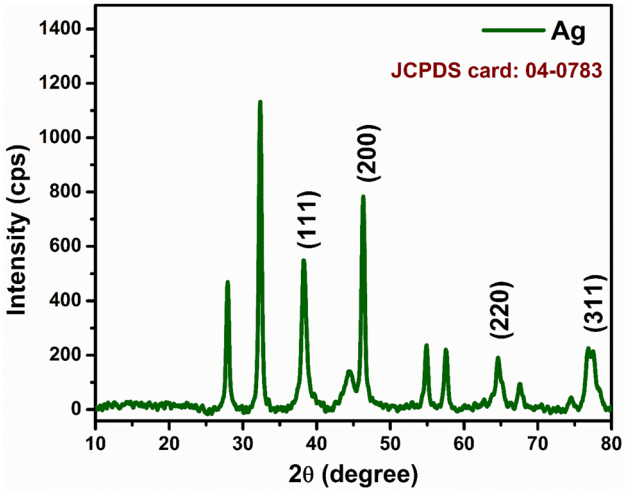

Figure 5: XRD pattern of *Z. mays* silk-fabricated AgNPs.

were found to have negative zeta potential, confirming the stability developed formulation [41]. Comparably, Erdogan et al. [42] observed that the zeta potential value of AgNPs from *Cynara scolymus* L. was about −32.3 ± 0.8 mV. The negative value might be due to the capping action of active metabolites present in the *Z. mays* extract.

In addition to this, the typical size of *Z. mays*-synthesized AgNPs was examined by DLS analysis (Figure 8) and determined an average particle size of 104 nm. Comparably, Murugan et al. [3] noted that the *Cymbopogon citrates*-synthesized Au nanoparticles had an average particle size of about 20 nm. Furthermore, Dwivedi and Gopal [43] observed that *Chenopodium album* L.-fabricated Ag and Au nanomaterials were stable under a wide pH range due to their high zeta potential.

3.3 Bio toxicity effect of CS extract and CS-AgNPs on *Ae. aegypti*

CS extract exhibited significant toxicity on dengue vector, *Ae. aegypti*, and the acquired LC_{50} values ranged from

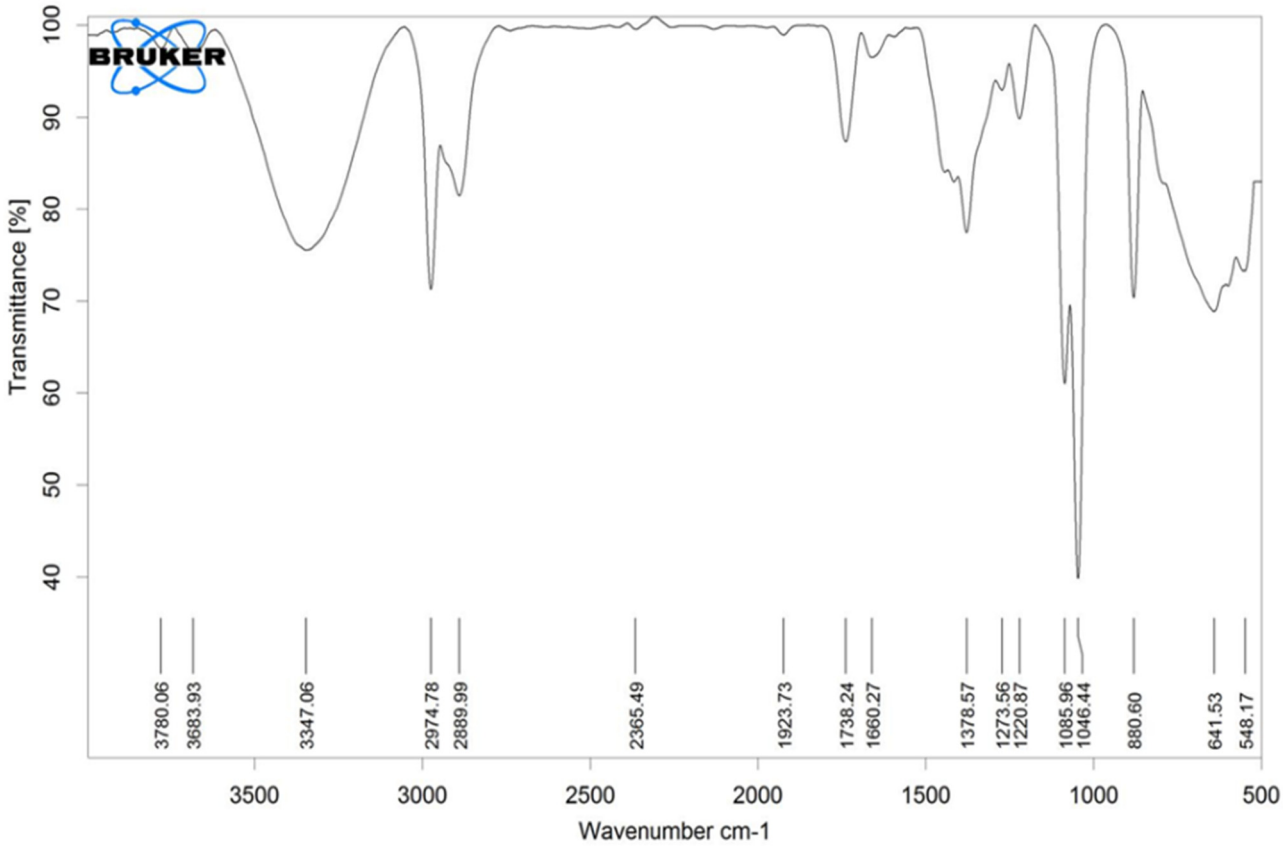

Figure 6: FTIR spectrum of *Z. mays* silk-fabricated AgNPs.

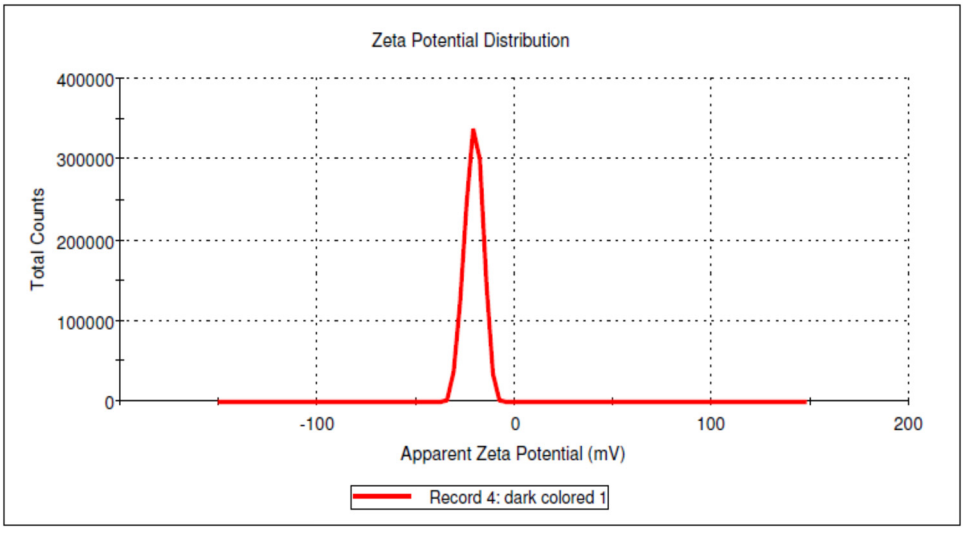

Figure 7: Zeta potential of *Z. mays* silk-fabricated AgNPs.

231.67 (I instar) to 447.89 $\mu g \cdot mL^{-1}$ (pupae) (Table 2). Moreover, CS-AgNPs were more toxic on *Ae. aegypti* when compared with CS extracts. Indeed, their LC_{50} values ranged from 2.35 (I instar) to 6.24 $\mu g \cdot mL^{-1}$ (pupae) (Table 3). To our knowledge, no reports on the larvicidal activity of CS extract and CS-fabricated AgNPs against *Ae. aegypti* have been reported. The current results were compared with other reports of plant extracts, for example, *Valoniopsis pachynema* (G. Martens) Børgesen extract showed high toxicity against *An. stephensi* with LC_{50} values ranging from

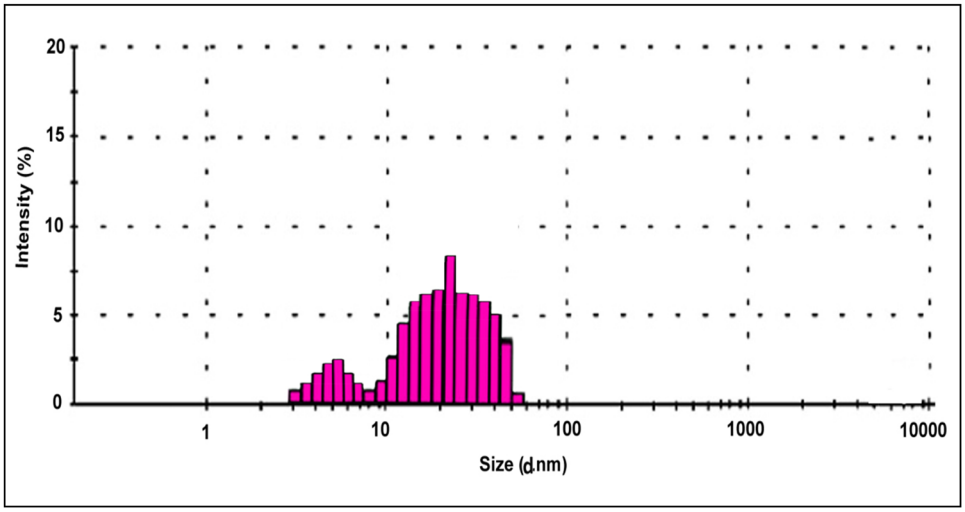

Figure 8: DLS spectrum of *Z. mays* silk-fabricated AgNPs.

Table 2: Biotoxicity of *Z. mays* silk methanolic extract against larvae and pupae of *Ae. aegypti*

Targets	LC_{50} (LC_{90})	95% confidence limit LC_{50} (LC_{90})		Regression equation	χ^2
		LCL	UCL		
Larva I	231.673 (527.357)	199.562 (259.425)	478.254 (598.380)	$x = 0.004$, $y = -1.004$	4.256 n.s
Larva II	265.993 (574.355)	235.559 (294.171)	518.859 (655.892)	$x = 0.004$, $y = -1.105$	2.492 n.s
Larva III	328.373 (690.093)	295.832 (363.747)	610.510 (815.790)	$x = 0.004$, $y = -1.163$	0.571 n.s
Larva IV	406.625 (796.961)	368.553 (457.805)	693.051 (969.806)	$x = 0.003$, $y = -1.335$	3.893 n.s
Pupae	447.894 (828.115)	406.448 (507.313)	719.525 (1009.230)	$x = 0.003$, $y = -1.510$	2.177 n.s

Control – no mortality; LC_{50} – lethal concentration killing 50% of the insects; LC_{90} – lethal concentration killing 90% of the insects; χ^2 – chi-square; n.s. – not significant ($\alpha = 0.05$).

Table 3: Biotoxicity of *Z. mays* silk-synthesized AgNPs against larvae and pupae of *Ae. aegypti*

Targets	LC_{50} (LC_{90})	95% confidence limit LC_{50} (LC_{90})		Regression equation	χ^2
		LCL	UCL		
Larva I	2.354 (6.450)	1.624 (2.902)	5.885 (7.214)	$x = 0.313$, $y = -0.736$	4.687 n.s
Larva II	3.064 (8.368)	2.280 (3.666)	7.620 (9.413)	$x = 0.024$, $y = -0.740$	2.782 n.s
Larva III	3.670 (10.354)	2.784 (4.348)	9.282 (11.974)	$x = 0.192$, $y = -0.704$	1.488 n.s
Larva IV	5.164 (11.471)	4.528 (5.740)	10.344 (13.137)	$x = 0.203$, $y = -1.049$	1.570 n.s
Pupae	6.240 (13.087)	5.616 (6.887)	11.666 (15.273)	$x = 0.187$, $y = -1.168$	2.005 n.s

Control – no mortality; LC_{50} – lethal concentration killing 50% of the insects; LC_{90} – lethal concentration killing 90% of the insects; χ^2 – chi-square; n.s. – not significant ($\alpha = 0.05$).

216.560 (larva I) to 359.868 $\mu g \cdot mL^{-1}$ (pupa), while for *An. sundaicus* they ranged from 188.871 to 311.860 $\mu g \cdot mL^{-1}$ [24]. Recently, Alshehri et al. [44] stated that *Heritiera fomes* Buch.-Ham leaf extract showed toxicity on *An. stephensi* and *Ae. aegypti*, in a dose-dependent manner.

3.4 Impact of CS-AgNPs on *Poecilia reticulata* predation

The predatory activity of *P. reticulate* fishes was calculated against I-IV instar larvae of *A. aegypti*. Guppy fish showed a high feeding activity in water containing

CS-fabricated AgNPs, indicating lack of intoxication effects on this nontarget species. In standard laboratory conditions, low doses of AgNPs were treated with water where the fishes were introduced, their predatory efficacy were 43.2% (I instar), 74% (II instar), 65.8% (III instar), and 39.5% (IV instar) after 24 h treatment. The predatory efficacy of *P. reticulate* was 32.2% (I), 52.8% (II), 43.8% (III), and 30.2% (IV instar) (Table 4). Similarly, Saleeza et al. [45] studied the feeding competence of both male and female guppies, *P. reticulate* on *Ae. aegypti*, *Ae. Albopictus*, and *Cx. quinquefasciatus*, and they reported that female guppies predate more mosquito larvae than male guppies. The predatory rates of female guppies were 121.3, 105.6, and 72.3, and male guppies were 98.6, 73.6, and 47.6 for *Ae. aegypti*, *Ae. albopictus*, and *Cx. quinquefasciatus*, respectively. The predatory efficiency of *P. reticulate* post-treatment with *Toddalia asiatica* (L.) Lam.-synthesized AgNPs were 89.75% and 74% against II and III instar larvae of *Cx. quinquefasciatus* [46].

3.5 Field application of CS extract and CS-AgNPs on *Ae. aegypti*

In the field, the application of CS extracts and AgNPs ($10 \times LC_{50}$) leads to the reduction of larval population into 10.61% and 5.16% after 72 h (Table 5). Similarly, the leaf extract of *Catharanthus roseus* (L.) G. Don led to *An. stephensi* larval reduction of 12.26%, 28.80%, and 79.46% after 24, 48, and 72 h post-treatment [47] and the field application of *Phyllanthus niruri* L. extract ($10 \times LC_{50}$) led to larval density reductions of 39.9%, 69.2%, and 100% after 24, 48, and 72 h, respectively [22]. Concerning AgNPs, Rajaganesh et al. [48] studied *Dicranopteris linearis* (Burm.fil.) Underw.-synthesized AgNPs ($10 \times LC_{50}$) led to 56.5%, 18.33%, and 100% of reduction after 24, 48, and 72 h, respectively. The bio-toxicity of AgNPs on *Ae. aegypti* may be due to the tiny size of nanomaterials that can easily penetrate the exoskeleton of insects and even individual cells, producing shedding and other physiological interferences [49].

3.6 Anti-biofilm activity of CS-AgNPs

In this research, we studied the anti-biofilm efficacy of CS-AgNPs against *S. aureus* and *S. epidermidis* testing five different concentrations ranging from 25 to 125 $\mu g \cdot mL^{-1}$. Results showed a maximum inhibitory effect (90% and 79% inhibition) at 125 $\mu g \cdot mL^{-1}$ on *S. aureus* and *S. epidermidis*, respectively (Table 6, Figure 9). Similarly, Patra and Baek [37] observed that corn silky hairs-fabricated AgNPs exhibited strong antibacterial effect on five various

Table 4: Predatory efficacy of *Poecillia reticulta* against dengue vector, *Ae. aegypti* post-treatment with 1 ppm of AgNPs (i.e., 1/3 of the LC_{50} calculated against first instar larvae of *Ae. aegypti*) (weighted generalized linear model, $P < 0.05$)

Treatment	Targets	Daylight (0–12 h)	Night time (12–24 h)	Total predation (*n*)	Total predation (%)
Standard conditions	I instar	70.6 ± 1.92	58.3 ± 1.58	128.9^{g}	32.2
	II instar	112.6 ± 1.14	98.6 ± 1.58	211.2^{c}	52.8
	III instar	93.4 ± 1.58	82.1 ± 1.92	175.5^{d}	43.8
	IV instar	67.4 ± 1.78	58.3 ± 1.58	120.9^{h}	30.2
Post-treatment with nanoparticles	I instar	94.6 ± 1.58	78.5 ± 1.92	173.1^{e}	43.2
	II instar	165.4 ± 1.51	130.6 ± 2.30	296.0^{a}	74.0
	III instar	152.6 ± 1.72	110.5 ± 1.94	263.1^{b}	65.8
	IV instar	87.5 ± 1.58	70.4 ± 1.92	157.9^{f}	39.5

Predation rates are mean ± SD of four replicates (1 fish vs 400 mosquitoes per replicate).
Control was clean water without *P. reticulata* fishes.
Within the column, mean values followed by the same letter are not significantly different (weighted generalized linear model, $P < 0.05$).

Table 5: Field reduction of *Ae. aegypti* larval populations post-treatment with *Z. mays* silk extract and AgNPs in water storage reservoirs

Larval density	*Z. mays* extract ($10 \times LD_{50}$)				*Z. mays*-fabricated silver nanoparticles ($10 \times LD_{50}$)			
	Before treatment	24 h	48 h	72 h	Before treatment	24 h	48 h	72 h
	79.33 ± 12.43^{d}	57.83 ± 11.75^{c}	27.5 ± 6.12^{b}	10.16 ± 4.62^{a}	73.00 ± 9.14^{d}	40.00 ± 9.81^{c}	18.00 ± 4.33^{b}	5.16 ± 2.71^{a}

Mean ± SD followed by different letter(s) are significantly different ($P < 0.05$).

Table 6: Impact of *Z. mays*-synthesized AgNPs on biofilm and EPS inhibition on *S. aureus* and *S. epidermidis*

Concentration ($\mu g \cdot mL^{-1}$)	Biofilm inhibition		EPS inhibition	
	S. aureus	*S. epidermidis*	*S. aureus*	*S. epidermidis*
25	17.78 ± 1.01^{e}	14.20 ± 0.99^{e}	15.08 ± 1.04^{e}	13.77 ± 0.73^{e}
50	38.75 ± 1.28^{d}	26.30 ± 1.04^{d}	$30.4 \pm 1.06d$	27.75 ± 1.12^{d}
75	67.47 ± 1.50^{c}	47.87 ± 1.55^{c}	46.90 ± 1.38^{c}	38.74 ± 1.51^{c}
100	78.79 ± 1.29^{b}	69.12 ± 1.00^{b}	66.04 ± 1.17^{b}	55.91 ± 0.77^{b}
125	90.01 ± 0.85^{a}	78.70 ± 1.35^{a}	79.95 ± 1.22^{a}	71.67 ± 0.89^{a}

Values were mean ± SD of three replicates.
Within a column mean values followed by the same letter(s) are not significantly different ($P < 0.05$).

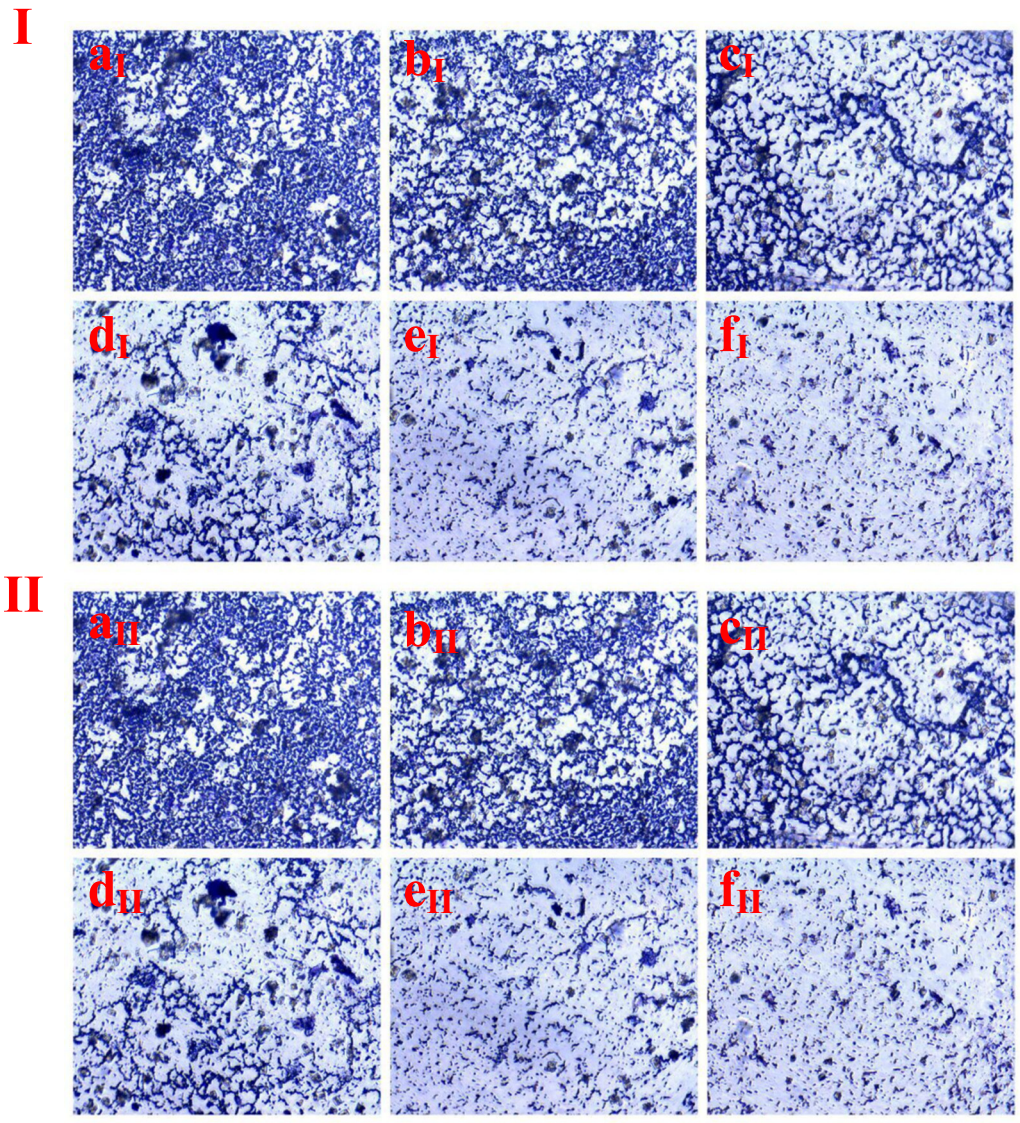

Figure 9: Light microscopic observation (40×) of *S. aureus* (I) and *S. epidermidis* (II) adhesion phases on the glass surfaces with different concentration ((a) control, (b) 25 $\mu g \cdot mL^{-1}$, (c) 50 $\mu g \cdot mL^{-1}$, (d) 75 $\mu g \cdot mL^{-1}$, (e) 100 $\mu g \cdot mL^{-1}$, (f) 125 $\mu g \cdot mL^{-1}$) of *Z. mays*-synthesized AgNPs against control which is indicative of glass surface with uniformly distributed cells stained with crystal violet.

bacterial pathogens with inhibition zones between 9.23 and 12.81 mm. The results of light microscopy examination revealed alteration in the cell membrane permeability and inhibition of DNA replication when compared with control, and the biofilm thickness was notably reduced after treatment with CS-AgNPs at 125 $\mu g \cdot mL^{-1}$ (Figure 9). Interestingly, when treated with CS-AgNPs, a lesser number of scattered cell aggregates in the biofilm have been observed. Overall, these results suggested that high doses of AgNPs increase the oxidative stress leading to bacterial cell detachment [50].

3.7 Quantification of EPS

Biofilm is formed by adhering complex communities that are encased within extracellular polymeric matrix. The EPS helps to protect the bacterial communities from oxidizing biocides, UV radiation, and antibiotics [51]. Therefore, disintegration of extra polymeric matrix paves way for assassination of biofilm. Herein, we studied the impact of CS-AgNPs on EPS formed by *S. aureus* and *S. epidermidis* within the biofilm. From the results, we observed a reduction of EPS formation in both *S. aureus* and *S. epidermidis* after treatment with different concentrations of AgNPs (Figure 9). Notably, the reduction of EPS observed at the concentration of 125 $\mu g \cdot mL^{-1}$ was of 79.95% and 71.67% *S. aureus* and *S. epidermidis*, respectively. The inhibition of biofilm formation and the reduction of EPS synthesis were dose dependent (Table 6). Rajkumari et al. [52] reported the anti-biofilm effect of gold nanoparticles against *Pseudomonas aeruginosa* and a reduction of EPS formation by 81.29%. Very recently, Alahmdi et al. [53] highlighted that the *Clitoria ternatea* L.-synthesized ZnO NPs significantly reduced EPS of both *E. coli* and *S. aureus* at 25–100 $g \cdot L^{-1}$, respectively.

4 Conclusion

Our research supported the use of CS, an important waste derived from corn crop production, as an effective and cheap capping agent to produce AgNPs acting as mosquitocidal agent. This formulation revealed to be eco-friendly since it improved the performance of the mosquito predator *P. reticulata*. In addition, the CS-fabricated nanoparticles revealed to be effective for the biofilm suppression, thus supporting their use as a sustainable antimicrobial agent. Thus, CS which is considered as an agricultural waste can be utilized for eco-friendly means of controlling deadly disease-causing mosquito larvae.

Acknowledgment: The authors thank Department of Zoology, Bharathiar University for providing the laboratory facilities.

Funding information: Authors state no funding involved.

Author contributions: Vasu Sujitha performed the experimental works and data compilation; Kadarkarai Murugan, Chellasamy Panneerselvam, and Al Thabiani Aziz analyzed the data and wrote the original draft; Fuad Abdullah Alatawi, Subrata Trivedi, and Zuhair M. Mohammedsaleh coordinated the work and discussed the results; Hatem A. Al-Aoh, Fayez M Saleh, and Suhair A. Bani-Atta contributed to formal analysis and data curation; and Giulia Bonacucina and Filippo Maggi reviewed and edited the manuscript. All authors have read and agreed to the published version of the manuscript.

Conflict of interest: Authors state no conflict of interest.

Data availability statement: The authors confirm that the data supporting the findings of this study are available in the article.

References

[1] Benelli G. Research in mosquito control: current challenges for a brighter future. Parasitol Res. 2015a;114:2801–5.
[2] Murugan K, Benelli G, Ayyappan S, Dinesh D, Panneerselvam C, Nicoletti M, et al. Toxicity of seaweed-synthesized silver nanoparticles against the filariasis vector *Culex quinquefasciatus* and its impact on predation efficiency of the cyclopoid crustacean *Mesocyclops longisetus*. Parasitol Res. 2015a;114:2243–53.
[3] Murugan K, Benelli G, Panneerselvam C, Subramaniam J, Jeyalalitha T, Dinesh D, et al. *Cymbopogon citratus* synthesized gold nanoparticles boost the predation efficiency of copepod *Mesocyclops aspericornis* against malaria and dengue mosquitoes. Exp Parasitol. 2015b;153:129–38.
[4] Alshehri MA, Aziz AT, Trivedi S, Panneerselvam C. Efficacy of chitosan silver nanoparticles from shrimp-shell wastes against major mosquito vectors of public health importance. Green Process Synth. 2020;9:675–84.
[5] Tesfazghi K, Hill J, Jones C, Ranson H, Worrall E. National malaria vector control policy: an analysis of the decision to scale-up larviciding in Nigeria. Health Policy Plan. 2016;31:9–101.
[6] Govindarajan M, Khater HF, Panneerselvam C, Benelli G. One-pot fabrication of silver nanocrystals using *Nicandra*

physalodes: A novel route for mosquito vector control with moderate toxicity on non-target water bugs. Res Vet Sci. 2016;107:95–101.
[7] Ahouansou CA, Houngbèmè GA, Mèdégan Fagla SR, Catteau L, Fagbohoun L, Kotchoni S, et al. Isolation and Identification of Two Triterpenes with Larvicidal Potential in *Launaea taraxacifolia* (Asteracae) on *Anopheles gambiae* by HPLC. Int J Curr Res Biosci Plant Biol. 2018;5(5):17–24.
[8] Pavela R, Bartolucci F, Desneux N, Lavoir AV, Canale A, Maggi F, et al. Chemical profiles and insecticidal efficacy of the essential oils from four *Thymus taxa* growing in central-southern Italy. Ind Crop Products. 2019;138:111460.
[9] Lakshmipathy R, Reddy BP, Sarada NC, Chidambaram K, Pasha SK. Watermelon rind-mediated green synthesis of noble palladium nanoparticles: catalytic application. Appl Nanosci. 2015;5(2):223–8.
[10] Roni M, Murugan K, Panneerselvam C, Subramaniam J, Hwang JS. Evaluation of leaf aqueous extract and synthesized silver nanoparticles using *Nerium oleander* against *Anopheles stephensi* (Diptera: Culicidae). Parasitol Res. 2013;112:981–90.
[11] Benelli G, Maggi F, Pavela R, Murugan K, Govindarajan M, Vaseeharan B, et al. Mosquito control with green nanopesticides: towards the One Health approach? A review of non-target effects. Env Sci Poll Res. 2018a;25:10184–206. doi: 10.1007/s11356-017-9752-4.
[12] Benelli G, Kadaikunnan S, Alharbi NS, Govindarajan M. Biophysical characterization of *Acacia caesia*-fabricated silver nanoparticles: effectiveness on mosquito vectors of public health relevance and impact on non-target aquatic biocontrol agents. Env Sci Poll Res. 2018b;25:10228–42. doi: 10.1007/s11356-017-8482-y.
[13] El Shafey AM. Green synthesis of metal and metal oxide nanoparticles from plant leaf extracts and their applications: A review. Green Process Synth. 2020;9(1):304–39.
[14] Aukkanit N, Kemngoen T, Ponharn N. Utilization of corn silk in low fat meatballs and its characteristics. Proc-Soc Behav Sci. 2015;197:1403–10.
[15] Carvalho ABL, Cleciana Alves Cruz CA, Freitas CLA, Aguiar JJS, Nunes PLWS, et al. Chemical profile, antibacterial activity, and antibiotic-modulating effect of the hexanic *Zea mays* L. silk extract (Poaceae). Antibiotics (Basel). 2019:8(1);22.
[16] Rumbaugh KP, Sauer K. Biofilm dispersion. Nat Rev Microbiol. 2020;18(10):571–86.
[17] Wang KJ, Zhao JL. Corn silk (*Zea mays* L.), a source of natural antioxidants with α-amylase, α- glucosidase, advanced glycation, and diabetic nephropathy inhibitory activities. Biomed Pharmacother. 2019;110:510–7.
[18] Garcia MI, Murúa FA, Díaz-Nieto LM, Acosta JC, Rios C, Cano AF, et al. Assessment of the predatory capacity on mosquito larvae of *Jenynsia multidentata* (Anablepidae) in presence of vegetation under laboratory conditions. Iheringia Sér Zool. 2018;1:1678–4766.
[19] Reen FJ, Gutiérrez-Barranquero JA, Parages ML, Gara FO. Coumarin: a novel player in microbial quorum sensing and biofilm formation inhibition. Appl Microbiol Biotechnol. 2018;102:2063–73.
[20] Murugan K, Nataraj D, Madhiyazhagan, Sujitha V, Chandramohan B, Panneerselvam C, et al. Carbon and silver nanoparticles in the fight against the filariasis vector *Culex quinquefasciatus*: genotoxicity and impact on behavioral traits of non-target aquatic organisms. Parasitol Res. 2016;115:1071–83.
[21] Sasidharan D, Namitha TR, Johnson SP, Jose V, Mathew P. Synthesis of silver and copper oxide nanoparticles using *Myristica fragrans* fruit extract: Antimicrobial and catalytic applications. Sustain Chem Pharm. 2020;16:100255.
[22] Hekmati M, Hasanirad S, Khaledi A, Esmaeili D. Green synthesis of silver nanoparticles using extracts of *Allium rotundum* L, *Falcaria vulgaris* Bernh, and *Ferulago angulate* Boiss, and their antimicrobial effects in vitro. Gene Rep. 2020;19:100589.
[23] Suresh U, Murugan K, Benelli G, Nicoletti M, Barnard DR, Panneerselvam C, et al. Tackling the growing threat of dengue: *Phyllanthus niruri*-mediated synthesis of silver nanoparticles and their mosquitocidal properties against the dengue vector *Aedes aegypti* (Diptera: Culicidae). Parasitol Res. 2015;114:1551–62.
[24] Sujitha V, Murugan K, Dinesh D, Pandiyan A, Aruliah R, Hwang JS, et al. Green-synthesized CdS nano-pesticides: Toxicity on young instars of malaria vectors and impact on enzymatic activities of the non-target mud crab *Scylla serrata*. Aquat Toxicol. 2017;188:100–8.
[25] Panneerselvam C, Murugan K, Roni M, Aziz AT, Suresh U, Rajaganesh R, et al. Fern-synthesized nanoparticles in the fight against malaria: LC/MS analysis of *Pteridium aquilinum* leaf extract and biosynthesis of silver nanoparticles with high mosquitocidal and antiplasmodial activity. Parasitol Res. 2016;115:997–1013.
[26] Murugan K, Vahitha R, Baruah I, Das SC. Integration of botanicals and microbial pesticides for the control of filarial vector, Culex quinquefasciatus. Ann Med Entomol. 2003;12:11–23.
[27] Mu H, Tang J, Liu Q, Sun C, Wang T, Duan J. Potent antibacterial nanoparticles against biofilm and intracellular bacteria. Sci Rep. 2016;6:18877.
[28] Stefanovic S, Hegde RS. Identification of a targeting factor for posttranslational membrane protein insertion into the ER. Cell. 2007;128(6):1147–59.
[29] Vanaraj S, Keerthana B, Preethi K. Biosynthesis, Characterization of silver nanoparticles using quercetin from Clitoria ternatea L to enhance toxicity against bacterial bioflm. J Inorg Organo Met Polym. 2017;27:1412–22.
[30] Dubois M, Gilles KA, Hamilton JK, Rebers PT, Smith F. Colorimetric method for determination of sugars and related substances. Anal Chem. 1956;28(3):350–6.
[31] Finney DJ. Probit analysis. London: Cambridge University; 1971. p. 68–78
[32] Abirami S, Priyalakshmi M, Soundariya A, Samrot AV, Saigeetha S, Emilin RR, et al. Antimicrobial activity, antiproliferative activity, amylase inhibitory activity and phytochemical analysis of ethanol extract of corn (*Zea mays* L.) silk. Curr Res Green SustaChem. 2021;4:100089.
[33] CarrilloW, Carpio, C, Morales D, Vilcacundo E, Alvarez M, Silva M. Content of Fatty acid in Corn (*Zea mays* L.) oil from Ecuador. Asian J Parma Clic Res. 2017;10(8):150–3.
[34] Barakat DA. Insecticidal and antifeedant activities and chemical composition of *Casimiroa edulis* La Llave & Lex (Rutaceae) leaf extract and its fractions against *Spodoptera littoralis* larvae. Australian J Basic Appl Sci. 2011;5(9):693–703.

[35] Rajkumar T, Sapi A, Das G, Debnath T, Ansari A, Patra JK. Biosynthesis of silver nanoparticle using extract of *Zea mays* (corn flour) and investigation of its cytotoxicity effect and radical scavenging potential. J Photochem Photobiol B: Biol. 2019;193:1–7.
[36] Hema JA, Malaka R, Muthukumarasamy NP, Sambandam A, Subramanian S, Sevanan M. Green synthesis of silver nanoparticles using *Zea mays* and exploration of its biological applications. IET Nanobiotechnol. 2016;10(5):288–94.
[37] Patra JK, Baek KH. Biosynthesis of silver nanoparticles using aqueous extract of silky hairs of corn and investigation of its antibacterial and anticandidal synergistic activity and antioxidant potential. IET Nanobiotechnol. 2016;10(5):326–33.
[38] Eren A, Baran MF. Green synthesıs, characterızatıon and antımıcrobıal actıvıty of sılver nanopartıcles (Agnps) from maıze (*Zea mays* L.). Applıed Ecol Envıron Res. 2019;17(2):4097–105.
[39] Chen Q, Liu G, Chen G, Chen T, Mi T. Green synthesis of silver nanoparticles with corn straw for the preparation of antibacterial paper. Bio Res. 2017;12(4):9063–74.
[40] Shankar SS, Rai A, Ahmad A, Sastry M. Rapid synthesis of Au, Ag, and bimetallic Au core-Ag shell nanoparticles using neem (*Azadirachta indica*) leaf broth. J Coll Interf Sci. 2004;275:496–502.
[41] Elamawi RM, Al-Harbi RE, Hendi AA. Biosynthesis and characterization of silver nanoparticles using *Trichoderma longibrachiatum* and their effect on phytopathogenic fungi. Egypt J Biol Pest Control. 2018;28:28. doi: 10.1186/s41938-018-0028-1.
[42] Erdogan O, Abbak M, Demirbolat GM, Birtekocak F, Aksel M, Pasa, et al. Green synthesis of silver nanoparticles via *Cynara scolymus* leaf extracts: The characterization, anticancer potential with photodynamic therapy in MCF7 cells. PLoS ONE. 2019;14(6):e0216496. doi: 10.1371/journal.pone.0216496.
[43] Dwivedi AD, Gopal K. Biosynthesis of silver and gold nanoparticles using Chenopodium album leaf extract. Colloids Surf A: Physicochem Eng Asp. 2010;369(1–3):27–33.
[44] Alshehri MA, Aziz AT, Trivedi S, Alanazi NA, Panneerselvam C, Baeshen R, et al. One-step synthesis of Ag nanoparticles using aqueous extracts from Sundarbans mangroves revealed high toxicity on major mosquito vectors and microbial pathogens. J Clust Sci. 2020;31:177–84.
[45] Saleeza SN, Norma-Rashid Y, Sofian-Azirun M. Guppies as predators of common mosquito larvae in Malaysia. Southeast Asian J Trop Med Public Health. 2014;45(2):299–308.
[46] Murugan K, Venus JS, Panneerselvam C, Bedini S, Conti B, Nicoletti M, et al. Biosynthesis, mosquitocidal and antibacterial properties of *Toddalia asiatica*-synthesized silver nanoparticles: do they impact predation of guppy *Poecilia reticulata* against the filariasis mosquito *Culex quinquefasciatus*? Env Sci Pollut Res Int. 2015e;22(21):17053–64.
[47] Panneerselvam C, Murugan K, Kovendan K, Kumar PM, Ponarulselvam S, Amerasan D, et al. Larvicidal efficacy of *Catharanthus roseus* Linn. (Family: Apocynaceae) leaf extract and bacterial insecticide *Bacillus thuringiensis* against *Anopheles stephensi* Liston. Asian Pac J Trop Med. 2013;6:847–53.
[48] Rajaganesh R, Murugan K, Panneerselvam C, Jayashanthini S, Aziz AT, Roni M, et al. Fern-synthesized silver nanocrystals: towards a new class of mosquito oviposition deterrents? Res Vet Sci. 2016;109:40–51.
[49] Roni M, Murugan K, Panneerselvam C, Subramaniam J, Nicoletti M, Madhiyazhagan P, et al. Characterization and biotoxicity of *Hypnea musciformis*-synthesized silver nanoparticles as potential eco-friendly control tool against *Aedes aegypti* and *Plutella xylostella*. Ecotoxicol Env Saf. 2015;121:31–8.
[50] Abinaya M, Vaseeharan B, Divya M, Sharmili A, Govindarajan M, Alharbi NS, et al. Bacterial exopolysaccharide (EPS)-coated ZnO nanoparticles showed high antibiofilm activity and larvicidal toxicity against malaria and Zika virus vectors. J Trace Elem Med Biol. 2018;45:93–103.
[51] Flemming HC, Wingender J. The biofilm matrix. Nat Rev Microbiol. 2010;8:623–33.
[52] Rajkumari J, Busi S, Vasu AC, Reddy P. Facile green synthesis of baicalein fabricated gold nanoparticles and their antibiofilm activity against *Pseudomonas aeruginosa* PAO1. Microb pathogenesis. 2017;107:261–9.
[53] Alahmdi MI, Syed K, Vanaraj S, Panneerselvam C, Mahnoud MAA, Mukhtar S, et al. *In Vitro* Anticancer and Antibacterial Activity of green synthesized ZnO NPs using *Clitoria ternatea* flower extract: Inhibits MCF-7 cell proliferation via intrinsic apoptotic pathway. J Inorg Organomet Polyme Mater. 2022;32:2146–59. doi: 10.21203/rs.3.rs-1269775/v1.